Nanoscale Advances

ROYAL SOCIETY OF CHEMISTRY

PAPER

View Article Online
View Journal | View Issue

Cite this: *Nanoscale Adv.*, 2021, **3**, 3085

ECM-mimicking nanofibrous scaffold enriched with dual growth factor carrying nanoparticles for diabetic wound healing†

Amritha Vijayan,‡[ab] Nanditha C. K.‡[ab] and G. S. Vinod Kumar *[a]

Polymeric nanofibrous scaffolds provide fine-tuned structures with inter-connecting pores resembling the natural extracellular matrix (ECM) in tissues, and show good potential in assisting the creation of artificial functional tissue. Additional application of growth factors helps to regulate the cellular behaviors and tissue assembly in the scaffolds, which eases the healing process. In this study, we synthesized an electrospun polymer scaffold system enriched with nanoparticles containing growth factors for accelerated healing of diabetic wounds. BSA nanoparticles were synthesized by cross-linking with PEG aldehyde. To free the amino group of BSA, heparin was conjugated by EDC/NHS chemistry. The angiogenic growth factors bFGF and VEGF were bound to heparin by electrostatic interaction. These nanoparticles were adsorbed on to electrospun collagen/PLGA/chitosan nanofibers. The synthesized nanofiber system was evaluated *in vitro* for its cell viability and proliferation. *In vivo* experiments conducted in a streptozotocin-induced diabetic mice model showed accelerated wound healing. The excellent healing efficiency of this ECM-mimicking nanofiber scaffold makes it a great candidate for therapeutic application in diabetic wounds.

Received 5th November 2020
Accepted 27th February 2021

DOI: 10.1039/d0na00926a

rsc.li/nanoscale-advances

Introduction

The electrospinning technique is effective in the preparation of polymeric fibrous non-woven extracellular matrix (ECM) analogue scaffolds.[1] Manufacture of nanofibers using the electrospinning technique is not only simple and cost-effective, but also provides an edge in terms of versatility. Electrospun nanofiber scaffolds provide an environment conducive to the viability, proliferation and migration of cells and also aid in the hemostasis phase of wound healing.[2–4] Nano-scale pores of electrospun mats thwart bacterial infection and enable high gas permeation which in turn prevents tissue degradation. Hence wound dressings in the form of nanofiber mats enhance compatibility paving the way for easy and faster wound repair and tissue regeneration.[5–7]

Nanofiber mats fabricated by the electrospinning technique exhibit a range of properties like easy and speedy wound repair. The fibrillar structural design and high porosity characteristic of electrospun mats offer the advantage of greater permeability, which in turn translates to shorter response time.[8] It also aids in biomimetics,[9] as it replicates both the structure and function of the native ECM. Synthetic polymer scaffolds have the ability to mimic the native ECM structure, while electrospun nanofibers of naturally occurring proteins like collagen provide a physiologically significant platform for the cells to proliferate and remodel.[10] Nanofiber scaffolds are pliable and, hence, can be applied to any part of the body, including the joints, with ease.[11]

Collagen, an ECM protein, found in abundance in mammals, especially at the sites of the skin, tendon, cartilage and bones is widely used in tissue engineering.[12] The biological origin, non-immunogenicity, superior biocompatibility as well as the biodegradable properties of collagen have made it a much-preferred biomaterial in a range of medical devices and tissue-engineered scaffolds. It serves as a sealant for vascular prostheses and dressing for wound repair.[13] Chitosan, a versatile polysaccharide, a natural biopolymer derived from chitin, due to its properties of good biocompatibility and appropriate biodegradability has emerged as an ideal biomaterial in the pharmaceutical and medical fields.[14–16] It can replace glycosaminoglycan, a major component of the natural extracellular matrix (ECM) for biomedical applications. Studies indicate that the excellent cell viability of the collagen–chitosan complex make it suitable for tissue engineering.[17] PLGA is an FDA approved polymer having excellent biocompatibility and biodegradability and degrades to release lactate, which promotes angiogenesis, stimulates collagen deposition and promotes closure of wounds.[18–20]

[a]*Chemical Biology, Nano Drug Delivery Systems (NDDS), Bio-Innovation Center (BIC), Rajiv Gandhi Centre for Biotechnology, Thycaud P.O, Thiruvananthapuram, Kerala, India-695014. E-mail: gsvinod@rgcb.res.in*

[b]*Research Centre, University of Kerala, Thiruvananthapuram, Kerala, India*

† Electronic supplementary information (ESI) available. See DOI: 10.1039/d0na00926a

‡ Equal first author contribution.

Skin regeneration is a dynamic process and several growth factors and cytokines are involved in modulating a series of cellular processes that are critical for healing.[21,22] However, in chronic wounds, the degradation or diminished expression of these growth factors impedes the generation of blood vessels, thereby preventing the unhindered transport of oxygen as well as nutrients to the wound site. The delivery of exogenous growth factors aids the regeneration of damaged skin tissues. Vascular endothelial growth factor (VEGF), a signal protein, which is produced by cells that stimulate blood vessel formation, plays an active role in the various processes of wound healing.[23] It not only promotes angiogenesis but stimulates wound healing *via* collagen deposition and epithelialization.[24–26] Basic fibroblast growth factor (bFGF) is another important growth factor involved in wound healing that promotes fibroblast proliferation and neovascularization, and is known for its anti-scarring properties.[27–29]

Several growth factors are clinically approved for topical use or as injections. But such applications at wound sites are limited by the lesser time of growth factor bioactivity and often require frequent administration which may cause adverse side effects.[30] Studies have shown that factors promoting tissue regeneration incorporated along with biomaterials have significantly enhanced wound healing in comparison to direct growth factor administration. Biomaterials act as a sustainable drug delivery agent for a longer time period and also protect the bioactive agents from protease degradation.[30] Electrospun ECM analogous nanofibrous scaffolds create a suitable platform for growth factor delivery. However, the delivery of growth factors using electrospun nanofiber scaffolds is not devoid of problems. Their incorporation into the nanofibers poses a challenge due to the presence of organic solvents in the electrospinning process that lead to their degradation. Growth factors functionalized on BSA nanoparticles using heparin as a small linker molecule are able to overcome this problem since albumin and heparin act as stabilizing agents and tend to protect growth factors.[31,32] BSA nanoparticles are also biocompatible, biodegradable, non-toxic and non-immunogenic.[33–35]

The simultaneous delivery of two growth factors bound to BSA nanoparticles using the native ECM-like nanofibrous scaffold as the delivery platform is an efficient solution for wound treatment and tissue regeneration. For the above-mentioned creation of the nanofiber scaffold, poly(ethylene glycol) (PEG) aldehyde cross-linked Bovine Serum Albumin (BSA) nanoparticles were prepared by the desolvation method and characterized by Transmission Electron Microscopy (TEM) and Dynamic Light Scattering (DLS). Heparin was conjugated to the free amino group of BSA by 1-ethyl-3-(3-dimethylaminopropyl) carbodiimide (EDC)/*N*-hydroxysuccinimide (NHS) chemistry and the efficiency of heparin-binding was calculated using a toluidine blue assay. To the heparin bound nanoparticles growth factors bFGF and VEGF were bound by electrostatic interaction between the arginine and lysine residues of the growth factors, and the negatively charged N- and O-sulphate groups of heparin. A poly(lactic-*co*-glycolic acid) (PLGA)–collagen–chitosan electrospun nanofiber scaffold was prepared and characterized by Fourier Transform Infra Red spectroscopy (FTIR) and Scanning Electron Microscopy (SEM). The growth factor carrying nanoparticles embedded in the PLGA–collagen–chitosan electrospun nanofiber scaffold were synthesised and evaluated *in vitro* and *in vivo* for wound healing and skin regeneration efficiency.

This technique helps in the combinatorial effect, and time bound release of the two growth factors is important in wound healing and also the uniform distribution of this into the entire nanofiber scaffold ensures and promotes the dynamic skin regeneration process.

In this study we reveal that complete epithelialization, a larger number of mature blood vessels, high density of fibroblasts, and increased mature collagen by day 15 suggest that BSA-GF nanoparticle embedded nanofibers (GF-NP-NFs) exhibit prominent wound healing capacity and a more effective treatment than the control group. The wound healing efficacy was further proved by the quantitative evaluation of the type I collagen, type III collagen and Ki-67 genes in the mRNA level from tissue sections. Higher gene expression of Type I and Type III collagen was found in the wounds treated with GF-NP-NFs as (group 4) compared to other groups.

Results and discussion

The addition of therapeutic bioactive molecules to the biopolymer matrix for enhanced wound repair is an emerging field of research with great potential.[36] It is known that growth factors have a therapeutic role in wound healing, but the uncontrolled application of growth factors can result in potential safety concerns.[37] They also have short half-life, are poorly absorbed due to enzymatic degradation and self-aggregation, and have poor bioavailability *in vivo*.[38] These factors call for an effective growth factor delivery system that is systemic, controlled and localized. Such a system is necessary for the development of successful products, reduction of side effects, improved bioavailability at the wound site and rate of delivery, relevant dose accumulation, and convenient mode of administration, improved patient compliance and conformational stability. The goal of synthesizing an ECM mimicking tissue-engineered scaffold is that the body should recognize it as "self", and use it to regenerate functional tissues.[39] Nanofibers are structurally similar to the native ECM and also serve as a reservoir and modulator for growth factors.[40]

Nanoparticle synthesis and characterization

Incorporation of growth factors into the nanofiber matrix is impeded due to solvent exposure during the electrospinning process, which may lead to the degradation of the growth factor.[41,42] The addition of bovine serum albumin has been reported to stabilize and protect the growth factors from organic solvents during preparation.[43] Heparin has a very significant binding affinity towards various biologically important proteins, such as growth factors and cytokines.[44] Hence the use of heparin to bind growth factors (GFs) to nanoparticles (NPs) is highly effective in drug delivery. The binding of heparin is also found to stabilize the growth factor molecules against

denaturation or proteolysis.[45,46] Moreover, heparin-binding also enhances the binding with cellular receptors.[47] Thus, heparins containing polymeric carriers are found to act as excellent drug delivery systems for growth factors. A nanoparticle–nanofiber complex was prepared to study the release of dual growth factors for wound healing.

Poly(ethylene glycol) (PEG) was converted to PEG aldehyde by the oxidation reaction.[48] The conversion of PEG to PEG aldehyde was confirmed by Fourier transform infrared spectroscopy (FTIR) (Fig. 1A). The characteristic band at 1738 cm^{-1} can be attributed to the aldehyde group of PEG aldehyde after its conversion. In this study, Bovine Serum Albumin (BSA) NPs were prepared by the desolvation method. In this process, ethanol is added continuously in a drop-wise manner. The solution is stirred continuously until it becomes turbid. While ethanol is added continuously, albumin is phase-separated due to its diminished water solubility. The albumin particles so formed are not stable enough and could re-dissolve after dispersion with water. Hence, the coacervates formed are hardened by crosslinking them with PEG aldehyde, where the amino moieties in the side chains of albumin are solidified by a condensation reaction with the aldehyde group of PEG aldehyde to form a Schiff base. The formation of PEG aldehyde cross-linked BSA nanoparticles was confirmed by FTIR (Fig. 1B). The characteristic peaks of amide A, amide I, and amide II bands at 3302.09 cm^{-1}, 1661.14 cm^{-1} and 1530.14 cm^{-}1 of BSA were present, whereas the characteristic peaks of PEG 1280, 947, and 843 cm^{-1} were also present. The peak at 1738 cm^{-1} of the aldehyde group disappears during the crosslinking process indicating the formation of a cross-linked nanoparticulate system. The strong peak observed at 1640 cm^{-1} belonging to C=N stretching shows the presence of the Schiff base linkage formed between aldehyde groups of PEG aldehyde and amino groups of BSA suggesting successful crosslinking.

Heparin immobilization of BSA nanoparticles was done by EDC/NHS chemistry, and the binding of heparin to the nanoparticle was confirmed by the toluidine blue assay. The amount of heparin bound to the nanoparticle was found to be 1.185 μg mg^{-1} of the nanoparticle. bFGF and VEGF are angiogenic growth factors which are important in the process of wound healing.[49,50] bFGF has been found to be involved in epithelialization, neovascularization and collagen synthesis at the wound site.[51–53] VEGF is involved in the degradation of basement membrane, angiogenesis and migration of vascular cells in the wound bed.[54,55] The growth factors bFGF and VEGF were bound to the heparinized BSA nanoparticles by electrostatic interactions between the heparin and growth factor molecules and their binding efficiency and release kinetics were studied by Enzyme-Linked Immunosorbent Assay (ELISA). The binding efficiency was 72% and 70% for bFGF and VEGF respectively.

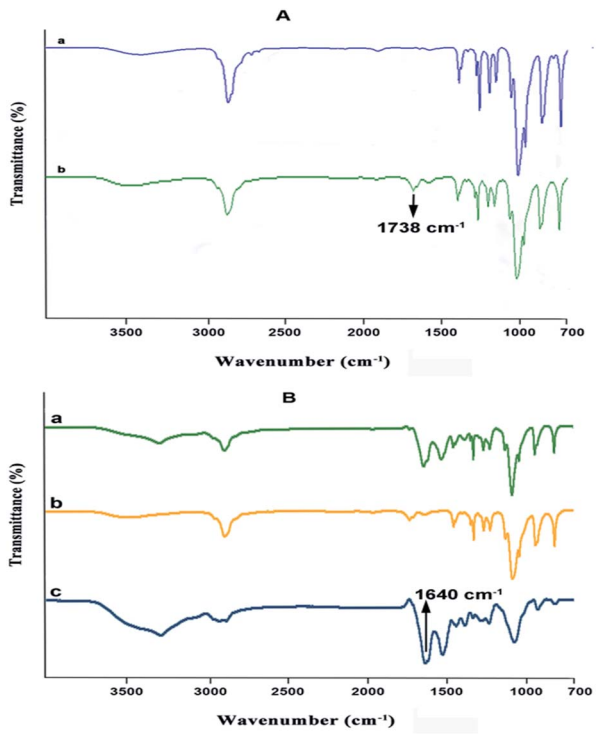

Fig. 1 (A) Fourier transform infrared spectroscopy (FTIR) spectrum of (a) poly(ethylene glycol) 1500 and (b) PEG aldehyde. (B) FTIR spectrum of (a) BSA, (b) PEG aldehyde and (c) cross-linked BSA PEG aldehyde nanoparticles.

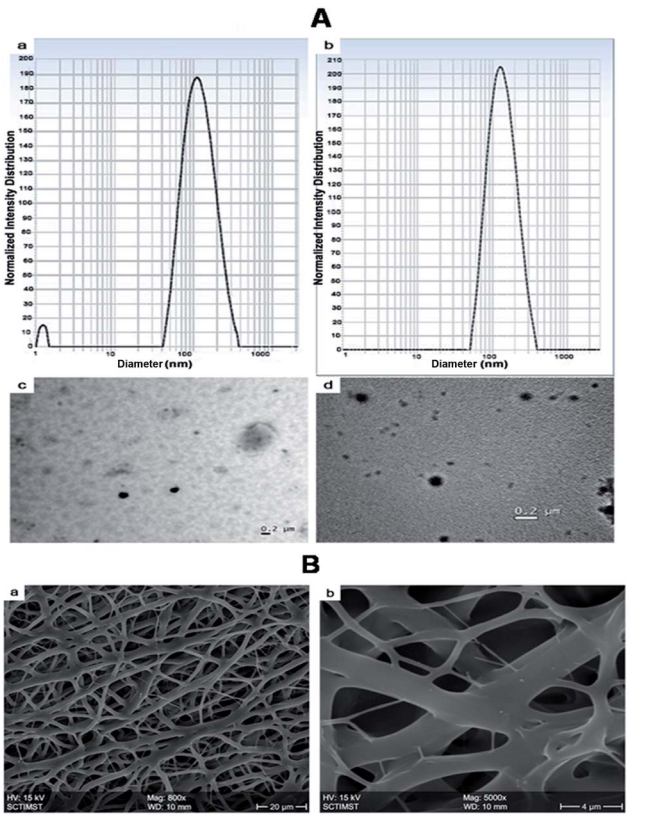

Fig. 2 (A) Nanoparticle size measurement using Dynamic Light Scattering (DLS) measurement of (a) NPs (BSA-PEG nanoparticles) and (b) GF NPs (growth factor coated BSA-PEG nanoparticles) and Transmission Electron Microscopy (TEM) images of (c) NPs and (d) GF NPs. (B) Scanning Electron Microscopy (SEM) image of PLGA–collagen–chitosan nanofibers (a) Mag: 800× and (b) Mag: 5000×.

The morphology and size of the nanoparticles were determined by DLS and TEM (Fig. 2A). The mean particle size of the nanoparticles was determined by Dynamic Light Scattering (DLS). The size of NPs (BSA-PEG nanoparticles) was found to be 113 ± 4.6 nm, whereas growth factor coated BSA-PEG nanoparticles (GF-NPs) had a size of 178 ± 6.34 nm.

Nanofiber scaffold fabrication and characterization

Electrospinning produces porous nanofiber mats, which when used for wound healing, aid in the permeation of oxygen from the external environment and volatilization of tissue fluid.[6] The morphology of the synthesized nanofibers was visualized by Scanning Electron Microscopy (Fig. 2B). The nanofibers were found to be of different sizes which may be due to the different polymers used in the fabrication. The steady release of growth factors from nanoparticles dispersed on the nanofiber surface helps to accelerate the skin regeneration process.

In the process of developing an efficient growth factor delivery system, it is important to study the release kinetics of the growth factor regarding its stability. In this study, the growth factors were released in a sustained manner over a period of 10 days. The release of growth factors from nanofibers mimics its release in the physiological environment and hence enhances the wound healing. Growth factor coated BSA nanoparticle embedded nanofibers (GF-NP-NFs) showed a continuous bFGF and VEGF release pattern over two weeks after a moderate burst release (Fig. 3A). The strong electrostatic interaction between heparin and the growth factors influences its release by prolonging the time required for it to reach the release media. This prolonged and sustained release of the growth factors helps in complete wound healing by assisting different healing stages.

Cytocompatibility assessment

The biocompatibility of nanoparticles in the nanofiber system for growth factor release was evaluated against *in vitro* cultures of HaCaT cells (Fig. 3B). The media in contact with the samples were collected at 24, 48 and 72 hours. The cells were treated with media incubated with the samples at different time points and were used to study the effect on HaCaT cell proliferation and survival. The system also showed no cytotoxicity on HaCaT cells, and the released growth factors maintained their bioactivity even when coated to the BSA-PEG nanoparticle embedded nanofiber matrix. It was found that the growth factor released from the nanoparticle embedded nanofiber system enhanced cell proliferation compared to the control and did not exhibit much cytotoxicity.

Keratinocytes are an essential cellular part of the epidermis. They play an important role in skin barrier maintenance and repair upon injury through the process of epithelialization. Re-epithelialization is an important phase in the process of wound healing and is characterized by increased keratinocyte proliferation and migration over the wound area.[56] The wound closure data obtained from the scratched wound healing assay are shown in Fig. 4A. For the cells treated with the samples of GF-NPs (growth factor coated BSA-PEG nanoparticles) and GF-

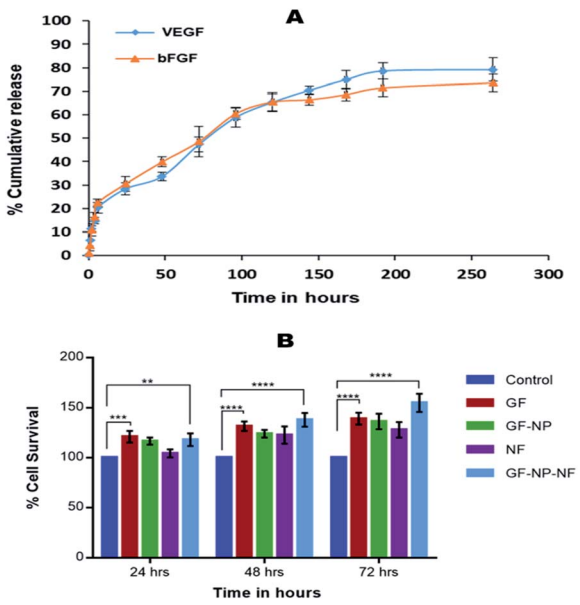

Fig. 3 (A) Release kinetics of bFGF and VEGF from GF-NP entrapped nanofibers. (B) MTT assay of HaCaT cells treated with (1) control (0.1 M PBS, pH 7.4), (2) GF (growth factors, VEGF and bFGF), (3) GF NPs (growth factor coated BSA-PEG nanoparticles), (4) NFs (PLGA–collagen–chitosan nanofibers), (5) GF-NP-NFs (growth factor coated BSA-PEG nanoparticle embedded nanofibers). Results expressed as mean ± SD ($n = 3$, $^*P < 0.05$, significance shown for GF and GF-NP-NF groups).

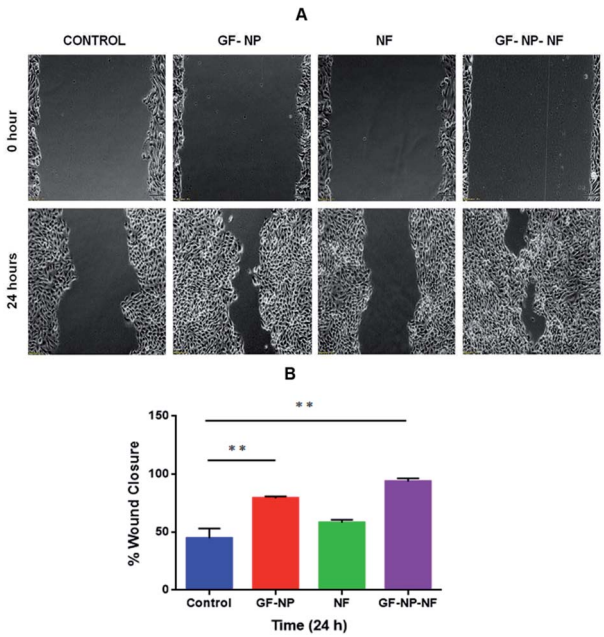

Fig. 4 (A) Scratch wound healing assay of HaCaT cells treated with (1) control (0.1 M PBS, pH 7.4), (2) GF-NPs (growth factor coated BSA-PEG nanoparticles), (3) NFs (PLGA–collagen–chitosan nanofibers), (4) GF-NP-NFs (growth factor coated BSA-PEG nanoparticle embedded nanofibers); images were obtained at 0 and 24 hours after wound creation. (B) Percentage wound closure at 24 hours. Results expressed as mean ± SD ($n = 3$, $^*P < 0.05$).

NP-NFs (growth factor coated BSA-PEG nanoparticle embedded nanofibers), it was observed that the wound healing activity at the 24 hour time point increased greatly when compared with the control. The results also showed that the GF-NP-NF treated sample showed significant healing effects in comparison to the control. The percentage wound closure (Fig. 4B) by the GF-NP (79%) and GF-NP-NF (93.5%) treated cells indicated much better wound healing action when compared to the control.

In the live/dead assay, the results were similar to that of MTT and scratch wound assay. The growth factor coated BSA-PEG nanoparticle embedded nanofibers (GF-NP-NFs) supported more proliferation and survival of HaCaT cells when compared to the control and other groups. When compared to the control, the NF (PLGA–collagen–chitosan nanofiber) group showed comparable cell survival and the GF-NP (growth factor coated BSA-PEG nanoparticle) group showed much more cell proliferation than the control and NF groups due to the action of growth factors (Fig. 5).

In vivo wound healing assessment

The dual growth factor carrying nanofibrous wound dressing was further evaluated *in vivo* on the streptozocin induced diabetic mice full-thickness skin defect model for its wound-healing ability. The rates of contraction of wounds treated with GF (group 1), GF-NP (group 2), NF (group 3), GF-NP-NF (group 4) and control groups were studied on day 0, 3rd day, 7th day and 15th day, respectively (Fig. 6A). On the 3rd day, all groups showed wound contraction to some extent, while GF-NP-NFs (group 4) displayed the largest area of contraction (61%) and GF (group 1) demonstrated about 54% contraction showing comparatively higher wound healing promotion effect when compared to the control and other groups. On the 7th day, GF-NP-NFs exhibited better therapeutic effect than the control and other groups. The wound contraction area of GF-NP-NFs was found to be 83% and that of the GF group was 78%. On the 15th day, even though all the groups exhibited very little wound area remaining, the GF-NP-NF group still had about approximately 5% better wound contraction than the remaining groups. The results from the GF-NP-NFs demonstrated better wound closure effect as shown by tracing the wound contraction area, which can be ascribed to the growth factor (bFGF, VEGF) release from the ECM-biomimetic PLGA/collagen/chitosan nanofiber scaffold.

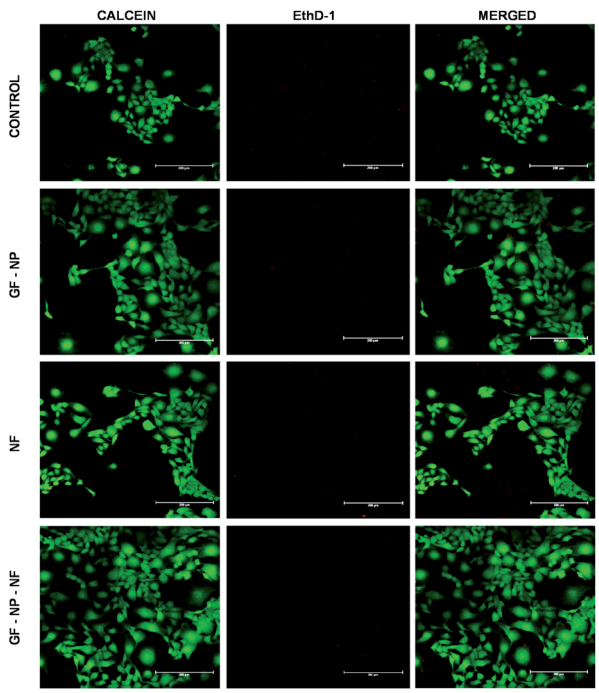

Fig. 5 Live/dead assay of HaCaT cells treated with (1) control (0.1 M PBS, pH 7.4), (2) GF-NPs (growth factor coated BSA-PEG nanoparticles), (3) NFs (PLGA–collagen–chitosan nanofibers), (4) GF-NP-NFs (growth factor coated BSA-PEG nanoparticle embedded nanofibers).

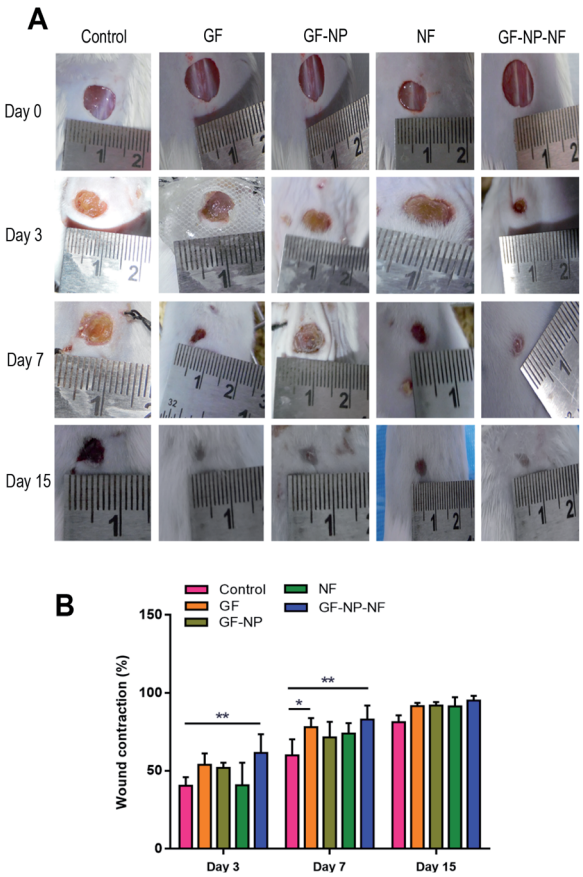

Fig. 6 VEGF and bFGF coated BSA-PEG nanoparticles embedded nanofiber accelerated wound healing in streptozocin induced diabetic mice. (A) Representative wound healing images of treatment groups tested on day 0, 3, 7 and 15. (B) Percentage of wound contraction tested on day 3, 7 and 15. Results expressed as mean ± SD ($n = 3$, $^*P < 0.05$).

Diabetic wounds are characterised by a degradative wound environment which limits the availability of local growth factors.[57] The nanofiber scaffold enriched with bFGF and VEGF growth factors (GF-NP-NF group) showed the best therapeutic effect during overall wound healing stages as the dual growth factors potentiate greater tissue regeneration by the combinatorial effect. The scaffold delivery system increases the growth

factor bioavailability window to the wound site with only a single application. The controlled gradual release of bFGF and VEGF growth factors from the ECM-biomimetic scaffold could accelerate the different wound healing stages and also stimulate fibroblast migration, granulation tissue formation and re-epithelialization. The ECM analogous electrospun nanofibrous scaffold improves wound contraction by providing a suitable platform for enhanced healing. Overall, the developed GF-NP-NFs showed a much better effect on the whole process of diabetic wound healing (Fig. 6B).

Post-wounding (day 15), the animals were sacrificed and their newly formed tissue was collected for histopathological examination. Hematoxylin and eosin-stained sections (H&E staining) (a–e) and Masson's trichome staining (f–j) were employed to assess the wound healing progress in different stages (Fig. 7A). By day 15, the formation of the basic structure of epithelium and dermis was observed in all groups. New blood vessel formation was observed more in GF-NP-NF treated groups when compared to all other groups (Fig. 7A(e), indicated by black arrows, Fig. S1† histomorphometrical analysis of angiogenesis). Predominantly, the maximum amount of new blood vessels, thickened epidermis and well-proliferated fibroblast demonstrated the best wound healing effect of GF-NP-NFs among the other groups possibly due to the gradual release of VEGF and bFGF and the ECM-like matrix provided by the scaffold. Masson's trichrome staining was done to assess collagen deposition. The GF, GF-NP and NF groups showed higher collagen deposition when compared to the control. The GF-NP-NF (group 4) treated tissue showed an increased mature collagen formation which indicates that the wound is progressing towards the remodelling phase.

In summary, an ECM mimicking nanofibrous scaffold embedded with dual growth factor (VEGF and bFGF) coated BSA-PEG nanoparticles enhanced wound closure in streptozotocin treated diabetic mouse. Gradual release of VEGF and bFGF to the wound site helped in angiogenesis, increased cell proliferation, collagen deposition and re-epithelialization. The wound healing efficacy was further proved by the quantitative evaluation of the type I collagen, type III collagen and Ki-67 genes in the mRNA level from tissue sections. Higher gene expression of type I and type III collagen was found in the wounds treated with GF-NP-NFs (group 4) compared to other groups. There was also a slight increase in the expression of Ki 67 in wounds treated with GF-NP-NFs, which might indicate the transition of the wound from the proliferative to the remodelling phase (Fig. 7B). Overall, these results suggested that bFGF and VEGF functionalized BSA-PEG nanoparticles carrying the ECM-biomimetic nanofiber scaffold significantly accelerated wound closure and tissue regeneration and provide a better treatment solution for diabetic wounds.

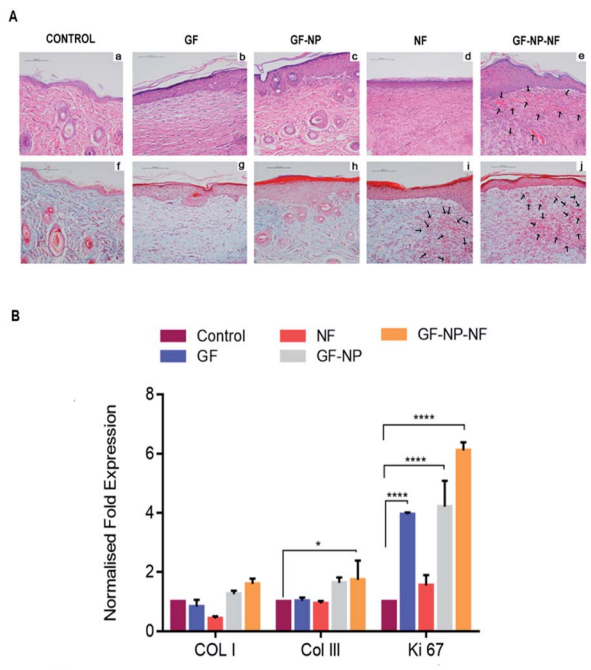

Fig. 7 (A) Representative images of H and E staining (a–e) and Masson's trichrome staining (f–j) of full thickness wounds 15 days post wounding (arrows indicate new capillaries). (B) Gene expression by qPCR of type I collagen, type III collagen and Ki-67 at day 15 of wound creation. Results expressed as mean ± SD ($n = 3$, $^*P < 0.05$).

Experimental

All the procedures for the experiments are given in the ESI.†

Conclusions

In this study, we synthesized an electrospun polymer scaffold system enriched with nanoparticles containing growth factors for accelerated healing of diabetic wounds. A combinatorial system containing dual growth factor functionalized nanoparticles embedded in a nanofiber was developed. The nanoparticle absorbed scaffold was characterized and evaluated *in vitro* for its cell viability and proliferation. It was tested for its wound healing efficacy in a streptozotocin induced diabetic mice model. It was found that the system enhanced the neovascularization of the wounded tissue, and collagen I, collagen III and Ki67 mRNA expression were also elevated which indicated the progression of the wound healing to the remodelling phase which in turn points to the enhanced and effective wound healing ability of the system. The excellent healing efficiency of this ECM-mimicking nanofiber scaffold makes it a great candidate for therapeutic application in diabetic wounds.

Animal studies

The animals (Swiss Albino Mice) were obtained from Rajiv Gandhi Centre for Biotechnology (RGCB) Animal Research Facility (Registration No. 326/GO/ReBiBt/S/2001/CPCSEA).

All animal experiments were carried out after the approval of Form B (Reference number: IAEC/285/GSV/2015) from Institutional Animal Ethics Committee (IAEC) at Rajiv Gandhi Centre for Biotechnology. The scientific intent was reviewed by the expert body of IAEC (consisting of eight members) for the approval of animal experiments. The experiments are carried

out based on the national rules and guidelines laid out by CPCSEA, New Delhi, India.

Funding

The authors are grateful to the Department of Biotechnology, New Delhi, for providing financial assistance for the research work and the University Grants Commission (UGC), New Delhi, for the Junior Research Fellowship to Amritha Vijayan and Nanditha C. K.

Conflicts of interest

The authors declare no competing financial interests.

Acknowledgements

The authors are grateful to Dr Vishnu Sunil Jaikumar, veterinary surgeon, Rajiv Gandhi Centre for Biotechnology (RGCB) for help with the *in vivo* study, Ms Rintu of RGCB for TEM analysis, Dr Arya Aravind of RGCB for histopathological analysis and the Sree Chitra Tirunal Institute for Medical Sciences and Technology (SCTIMST) Trivandrum for SEM analysis.

Notes and references

1 S. Y. Chew, Y. Wen, Y. Dzenis and K. W. Leong, *Curr. Pharm. Des.*, 2006, **12**(36), 4751–4770.
2 A. Memic, T. Abudula, H. S. Mohammed, K. J. Navare, T. Colombani and S. A. Bencherif, *ACS Appl. Bio Mater.*, 2019, **2**, 952–969.
3 S. Chen, B. Liu, M. A. Carlson, A. F. Gombart, D. A. Reilly and J. Xie, *Nanomedicine*, 2017, **12**, 1335–1352.
4 Y. Zhang, C. T. Lim, S. Ramakrishna and Z.-M. Huang, *J. Mater. Sci.: Mater. Med.*, 2005, **16**, 933–946.
5 Y. J. Son, J. W. Tse, Y. Zhou, W. Mao, E. K. F. Yim and H. S. Yoo, *Biomater. Sci.*, 2019, **7**, 4444–4471.
6 K. Ye, H. Kuang, Z. You, Y. Morsi and X. Mo, *Pharmaceutics*, 2019, **11**, 182.
7 C. Zhang and S. Yu, *Mater. Horiz.*, 2016, **3**, 266–269.
8 H. Gao, Z. Zhong, H. Xia, Q. Hu, Q. Ye, Y. Wang, L. Chen, Y. Du, X. Shi and L. Zhang, *Biomater. Sci.*, 2019, **7**, 2571–2581.
9 M. Berthet, Y. Gauthier, C. Lacroix, B. Verrier and C. Monge, *Trends Biotechnol.*, 2017, **35**, 770–784.
10 S. A. Sell, P. S. Wolfe, K. Garg, J. M. McCool, I. A. Rodriguez and G. L. Bowlin, *Polymers*, 2010, **2**(4), 522–553.
11 S. Liao, F. Z. Cui, W. Zhang and Q. L. Feng, *J. Biomed. Mater. Res., Part B*, 2004, **69**, 158–165.
12 Z. Chen, X. Mo, C. He and H. Wang, *Carbohydr. Polym.*, 2008, **72**, 410–418.
13 G. W. Bos, A. A. Poot, B. Beugeling, W. G. van Aken and J. Feijen, *Arch. Physiol. Biochem.*, 1998, **106**, 110–115.
14 K. Xu, Z. Wang, J. A. Copland, R. Chakrabarti and S. J. Florczyk, *Biomaterials*, 2020, **254**, 120126.
15 Zhao, S. Yu, B. Sun, S. Gao, S. Guo and K. Zhao, *Polymers*, 2018, **10**, 462.
16 A. Shavandi, T. H. Silva, A. A. Bekhit and A. E. A. Bekhit, *Biomater. Sci.*, 2017, **5**, 1699–1735.
17 J. Huang, J. Ren, G. Chen, Z. Li, Y. Liu, G. Wang and X. Wu, *Mater. Sci. Eng., C*, 2018, **89**, 213–222.
18 K. Chereddy, G. Vandermeulen and V. Préat, *Wound Repair Regen.*, 2016, **24**, 223–236.
19 E. Porporato, V. L. Payen, C. J. D. Saedeleer, V. Préat, J. Thissen, O. Feron and P. Sonveaux, *Angiogenesis*, 2012, **15**, 581–592.
20 X. Hu, Y. Feng, G. Xiang, W. Lei and L. Wang, *J. Mater. Chem. B*, 2018, **6**, 2274–2288.
21 F. Zarei and M. Soleimaninejad, *Artif. Cells, Nanomed., Biotechnol.*, 2018, **46**, 906–911.
22 M. Zubair and J. Ahmad, *Rev. Endocr. Metab. Disord.*, 2019, **20**, 207–217.
23 K. E. Johnson and T. A. Wilgus, *Adv. Wound Care*, 2014, **3**, 647–661.
24 P. Bao, A. Kodra, M. Tomic-Canic, M. S. Golinko, H. P. Ehrlich and H. Brem, *J. Surg. Res.*, 2009, **153**, 347–358.
25 Chereddy, A. Lopes, S. Koussoroplis, V. Payen, C. Moia, H. Zhu, P. Sonveaux, P. Carmeliet, A. Rieux, G. Vandermeulen and V. Préat, *Nanomedicine*, 2015, **11**, 1975–1984.
26 K. Lee, E. A. Silva and D. J. Mooney, *J. R. Soc., Interface*, 2011, **8**, 153–170.
27 S. Akita, K. Akino and A. Hirano, *Adv. Wound Care*, 2013, **2**, 44–49.
28 A. Chen, W. Huang, L. Wu, Y. An, T. Xuan, H. He, M. Ye, L. Qi and J. Wu, *ACS Appl. Bio Mater.*, 2020, **3**, 3039–3048.
29 Losi, E. Briganti, C. Errico, A. Lisella, E. Sanguinetti, F. Chiellini and G. Soldani, *Acta Biomater.*, 2013, **9**, 7814–7821.
30 A. Nurkesh, A. Jaguparov, S. Jimi and A. Saparov, *Front. Cell Dev. Biol.*, 2020, **8**, 638.
31 Rohman, S. C. Baker, J. Southgate and N. R. Cameron, *J. Mater. Chem.*, 2009, **19**, 9265–9273.
32 P. Olczyk, Ł. Mencner and K. Komosinska-Vassev, *BioMed Res. Int.*, 2015, **2015**, 549417.
33 A. O. Elzoghby, W. M. Samy and N. A. Elgindy, *J. Controlled Release*, 2012, **157**, 168–182.
34 S. Azizian, A. Hadjizadeh and H. Niknejad, *Carbohydr. Polym.*, 2018, **202**, 315–322.
35 Z. Wang, Z. Wang, W. W. Lu, W. Zhen, D. Yang and S. Peng, *NPG Asia Mater.*, 2017, **9**, e435.
36 J. Jee, R. Pangeni, S. K. Jha, Y. Byun and J. W. Park, *Int. J. Nanomed.*, 2019, **14**, 5449–5475.
37 R. Subbiah and R. E. Guldberg, *Adv. Healthcare Mater.*, 2019, **8**, e1801000.
38 A. C. Mitchell, P. S. Briquez, J. A. Hubbell and J. R. Cochran, *Acta Biomater.*, 2016, **30**, 1–12.
39 Nour, N. Baheiraei, R. Imani, M. Khodaei, A. Alizadeh, N. Rabiee and S. M. Moazzeni, *J. Mater. Sci.: Mater. Med.*, 2019, **30**, 120.
40 C. P. Barnes, S. A. Sell, E. D. Boland, D. G. Simpson and G. L. Bowlin, *Adv. Drug Delivery Rev.*, 2007, **59**, 1413–1433.
41 S. Liu, M. Qin, C. Hu, F. Wu, W. Cui, T. Jin and C. Fan, *Biomaterials*, 2013, **34**, 4690–4701.

42 M. Sekyi, J. Taussig and M. J. Kipper, *Macromol. Biosci.*, 2016, **16**, 371–380.
43 T. W. King and C. W. Patrick Jr, *J. Biomed. Mater. Res.*, 2000, **51**, 383–390.
44 Y. K. Joung, J. W. Bae and K. D. Park, *Expert Opin. Drug Delivery*, 2008, **5**, 1173–1184.
45 Vijayan, P. P. James, C. K. Nanditha and G. S. V. Kumar, *Int. J. Nanomed.*, 2019, **14**, 2253–2263.
46 A. Vijayan, A. Sabareeswaran and G. S. V. Kumar, *Sci. Rep.*, 2019, **9**, 1–12.
47 Faham, R. E. Hileman, J. R. Fromm, R. J. Linhardt and D. C. Rees, *Science*, 1996, **271**, 1116–1120.
48 M. Zhang, X. H. Li, Y. D. Gong, N. M. Zhao and X. F. Zhang, *Biomaterials*, 2002, **23**, 2641–2648.
49 N. Sun, B. Ning, K. M. Hansson, A. C. Bruce, S. A. Seaman, C. Zhang, M. Rikard, C. A. DeRosa, C. L. Fraser, M. Wågberg, R. Fritsche-Danielson, J. Wikström, K. R. Chien, A. Lundahl, M. Hölttä, L. G. Carlsson, S. M. Peirce and S. Hu, *Sci. Rep.*, 2018, **8**, 17509.
50 H. Lai, C. Kuan, H. Wu, J. Tsai, T. Chen, D. Hsieh and T. Wang, *Acta Biomater.*, 2014, **10**, 4156–4166.
51 S. Werner and R. Grose, *Physiol. Rev.*, 2003, **83**, 835–870.
52 S. M. McCarty and S. L. Percival, *Adv. Wound Care*, 2013, **2**, 438–447.
53 J. Liu, H. Zheng, X. Dai, S. Sun, H. Machens and A. F. Schilling, *J. Tissue Sci. Eng.*, 2017, **8**, 193–196.
54 R. D. Daliano, O. M. Tepper, C. R. Pelo, K. A. Bhatt, M. Callaghan, N. Bastidas, S. Bunting, H. G. Steinmetz and G. C. Gurtner, *Am. J. Pathol.*, 2004, **164**, 1935–1947.
55 P. Bao, A. Kodra, M. Tomic-Canic, M. S. Golinko, H. P. Ehrlich and H. Brem, *J. Surg. Res.*, 2009, **153**, 347–358.
56 R. K. Sivamani, *Adv. Wound Care*, 2014, **3**, 476–481.
57 J. Berlanga-Acosta, Y. Mendoza-Mari, A. Garcia-Ojalvo, J. A. Acosta-Buxado, M. Fernandez-Mayola and G. Guillen Nieto, *Integr. Mol. Med.*, 2019, **6**(1), 1–7.